

Application of the Geselowitz Relationship to the Murine Conductance Catheter

Erik R. Larson and John A. Pearce, *Senior Member, IEEE*

Abstract—Conductance catheters are known to have a nonuniform spatial sensitivity due to the distribution of the electric field. The Geselowitz relation is applied to the murine conductance catheter using a finite element model to determine catheter’s spatial sensitivity in uniform media. Further analysis of FEM numerical modeling results using the Geselowitz relation provides a true measure of parallel conductance in a simplified murine left ventricle for assessment of the admittance method and hypertonic saline techniques. The spatial sensitivity of blood conductance (G_b) is determined throughout the cardiac cycle. G_b is converted to volume using Wei’s equation to determine if the presence of myocardium alters the nonlinear relationship through changes to the electric field shape. Results show that the admittance method correctly calculates G_b in comparison to the Geselowitz relation, and that the relationship between G_b and volume is accurately fit using Wei’s equation.

I. INTRODUCTION

BIOIMPEDANCE measurements are often used to indirectly monitor physiologic processes such as respiration or blood volume. The conductance catheter technique was introduced by Baan *et al* [1] as a method to continuously measure left ventricular (LV) volume. The technique places a multi electrode catheter in the LV and measures the conductance using a tetrapolar measurement. Since the resulting conductance cannot be directly converted to volume, stroke volume measurements are typically used in the conversion of conductance to volume.

Blood, muscle and surrounding tissues are included in the conductance measurement as the electric field extends outside the LV blood pool [2, 3]. Conductance outside the LV blood pool, referred to as parallel conductance, causes error in the volume measurement.

Plethysmography instruments commonly measure the magnitude of impedance, neglecting the complex nature of tissues. Cardiac and skeletal muscle exhibit significant and observable permittivity at frequencies above 2 kHz [4, 5], which is an important consideration in plethysmography measurements.

Manuscript received March 14, 2012. This work was supported in part by the T.L.L. Temple Foundation.

E. R. Larson is a PhD candidate in Electrical Engineering at the The University of Texas at Austin, (e-mail: Larson@ece.utexas.edu).

J. A. Pearce is Temple Foundation Professor of Electrical and Computer Engineering at the University of Texas at Austin, 1 University Station, Austin, TX 78712. (telephone: 512-471-4984; fax: 512-471-3652; e-mail: jpearce@mail.utexas.edu).

Muscle’s high permittivity is most likely due to the transmembrane charge distribution. Charge is electrochemically bound to the membrane and forms a dipole which reacts to the application of time-varying electric fields.

Two techniques are commonly used to remove parallel conductance: 1) the hypertonic saline method and 2) the admittance method [6].

The hypertonic saline technique injects a small saline bolus into the jugular vein. As the bolus enters the LV, the high saline conductivity increases the measured conductance from the LV catheter while the SV is unchanged. End diastolic (ED) and end systolic (ES) conductance are used to project the parallel conductance.

The admittance method uses the complex nature of muscle to remove parallel conductance [6]. Measured admittance consists of three components, $Y = G_b + G_m + j\omega C_m$, where G_b is the conductance of blood, G_m is the conductance of muscle and ωC_m is the susceptance of muscle. Since the imaginary component arises solely from the muscle, the conductivity to permittivity ratio of muscle can be used to isolate blood conductance, $G_b = Re\{Y\} - (\sigma_m/\omega\epsilon_m)Im\{Y\}$.

Finite element analysis of plethysmography measurements is normally performed through calculation of the measured impedance, ignoring the spatial sensitivity of the measurement. Tetrapolar measurements exhibit complex sensitivity fields due to separation of the current carrying and voltage sensing electrodes. This paper addresses the spatial distribution of the measurement sensitivity.

II. METHODS

A. Impedance Formulation

Electrical properties are commonly defined with respect to a bulk measurement. A medium with finite conductivity and permittivity is modeled as a parallel resistor-capacitor network. Electric conductance, G , and capacitance, C , are defined as,

$$G = \frac{I}{V} = \frac{\iint_S \sigma \mathbf{E} \cdot d\mathbf{S}}{\int_b^a \mathbf{E} \cdot d\mathbf{L}} = \sigma F \quad (1)$$

and

$$C = \frac{Q}{V} = \frac{\iint_S \epsilon \mathbf{E} \cdot d\mathbf{S}}{\int_b^a \mathbf{E} \cdot d\mathbf{L}} = \epsilon F, \quad (2)$$

where I is the applied current [A], V is the measured voltage [V], Q is the charge [C], σ is the conductivity [S/m], ϵ is the permittivity [F/m] and \mathbf{E} is the electric field [V/m]. The surface S is any complete cross section between the current carrying electrodes and the line integral is any path between the voltage sensing electrodes.

This bulk definition may lead one to incorrectly conclude that the measurement is confined to the region between the equipotential surfaces formed by the voltage sensing electrodes [7]. Property variations between each pair of current-carrying and voltage-sensing electrodes contribute significantly to the total measurement. Another definition of impedance is necessary to quantify the spatial variations to the total measurement.

The relationship between the measured impedance and the local properties in a domain has previously been explored for the tetrapolar measurement [8, 9]. These derivations used a volume conductor model. Here we expand the derivation to semiconducting dielectrics. We first define a region with finite conductivity, σ , and permittivity, ϵ . Four electrodes are placed on the surface of the medium. The current, I , is applied between terminals A and B which results in the electric potential distribution $\varphi(\mathbf{r})$, where \mathbf{r} is the location. Alternatively, applying the same current between electrodes C and D results in the potential distribution $\psi(\mathbf{r})$. The measured impedance is the same under linear conditions, due to reciprocity, if the current and potential electrodes are swapped. This is only valid for the case where the positive current electrode is swapped with positive voltage electrode and the negative current electrode for the negative voltage electrode.

$$\mathbf{Z} = \frac{\varphi_{AB}}{I} = \frac{\psi_{CD}}{I} \quad (3)$$

This derivation closely follows Lehr's method, only we substitute the combined translational and displacement current densities, $\mathbf{J}^* = (\sigma + j\omega\epsilon)\mathbf{E}$, rather than just the translational current, $\mathbf{J} = \sigma\mathbf{E}$. Substituting $\psi(\sigma + j\omega\epsilon)\mathbf{E}_\varphi$ into the divergence theorem, and working toward a formulation of the measured impedance.

$$\begin{aligned} \iiint_V \psi(\nabla \cdot [(\sigma + j\omega\epsilon)\mathbf{E}_\varphi]) + (\sigma + j\omega\epsilon)\mathbf{E}_\varphi \cdot \nabla\psi \, dv \\ = \oint_S \psi(\sigma + j\omega\epsilon)\mathbf{E}_\varphi \cdot d\mathbf{s} \end{aligned} \quad (4)$$

Since there are no sources within the medium, $\nabla \cdot [(\sigma + j\omega\epsilon)\mathbf{E}_\varphi] = 0$.

$$\iiint_V (\sigma + j\omega\epsilon)\mathbf{E}_\varphi \cdot \nabla\psi \, dv = \oint_S \psi(\sigma + j\omega\epsilon)\mathbf{E}_\varphi \cdot d\mathbf{s} \quad (5)$$

We can neglect the normal component of the electric field on the surface at all points other than the applied current source. Assuming the current is supplied by a perfect conductor, we are left only with the applied current and potential.

$$\iiint_V (\sigma + j\omega\epsilon)\mathbf{E}_\varphi \cdot \nabla\psi \, dv = \varphi_A I - \varphi_B I = \varphi_{AB} I \quad (6)$$

If we divide both sides of the equation by I^2 and substitute \mathbf{E}_ψ for $\nabla\psi$,

$$\mathbf{Z} = \iiint_V \frac{(\sigma + j\omega\epsilon)\mathbf{E}_\varphi \cdot \mathbf{E}_\psi}{I^2} \, dv = \frac{\varphi_{AB}}{I} \quad (7)$$

We can manipulate this equation to aid its interpretation by formulating it in terms of the combined translational and displacement current densities, \mathbf{J}_φ^* and \mathbf{J}_ψ^* , rather than the electric fields.

$$\mathbf{Z} = \iiint_V \frac{\mathbf{J}_\varphi^* \cdot \mathbf{J}_\psi^*}{(\sigma + j\omega\epsilon)I^2} \, dv \quad (8)$$

This equation reflects the measured impedance as would be observed in a tetrapolar configuration and can be applied to a domain with non uniform properties. Local integrations of impedance only reflect the regions true impedance in domains oriented electrically in series. It is not valid for local integrations in parallel or mixed models since only part of the current is located in each domain, but the integration over the entire domain remains valid.

Conductivity and permittivity add in parallel. It is therefore best to analyze results in terms of admittance, \mathbf{Y} , rather than impedance. If we multiple equation (8) by \mathbf{Y}^2 the result is,

$$\mathbf{Y} = \iiint_V \frac{\mathbf{J}_\varphi^* \cdot \mathbf{J}_\psi^*}{(\sigma + j\omega\epsilon)V^2} \, dv, \quad (8)$$

where V is the difference in potential between the measurement electrodes.

Analysis of finite element models calculates blood and muscle conductance using two methods. First, the bulk admittance measurement is used with the admittance method to separate blood and muscle conductance, as would be done experimentally. Second, integration of the $\text{Re}\{\mathbf{Y}\}$, from the Geselowitz relation, over blood and muscle subdomains calculates blood and muscle conductance separately. The resulting values of each method are compared.

G_b is converted to volume using Wei's equation [10]. Although finite element models have previously been used to validate Wei's equation in an insulated cylinder, this model includes the surrounding muscle.

B. Finite Element Models

A tetrapolar mouse catheter is first analyzed in a uniform media to determine the distribution of the sensitivity field. Catheter dimensions are based on Scisense (London, Ontario) mouse catheters.

The catheter is then placed in a simple cylinder model of the mouse left ventricle. Dimensions of the mouse LV are based on ultrasound measurements [11]. The outer muscle wall dimensions are held constant and the radius of the blood cylinder is varied to simulate volumes throughout the cardiac cycle. Calculations of G_b using the admittance method and the Geselowitz relationship are compared, and G_b is converted to volume using Wei's equation.

The resulting geometry of the mouse LV is shown in Fig. 1

at diastole. Systole corresponded to a volume of 16 μL and diastole to 48 μL . Further analysis is performed over a range of 15 to 60 μL .

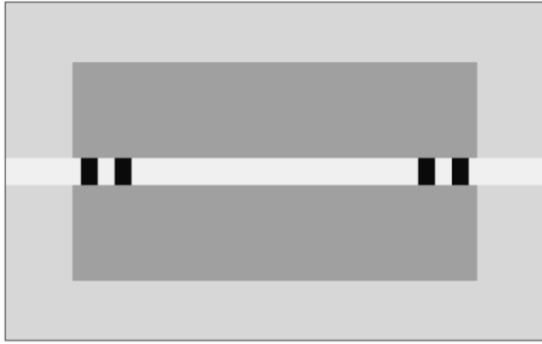


Fig. 1. Mouse conductance catheter in a cylindrical model of the mouse LV.

Analysis of the sensitivity distribution in the blood cavity is performed through computation of the contribution each segmental volume makes to the total G_b . This is performed by integrating the impedivity-sensitivity product, the integrand in equation 8, over cylinders with a radius that extends to the endocardium and a height of 0.25 mm.

Values used for conductivity and permittivity for each domain are shown in Table I. Blood and muscle properties are from measurements by Raghavan *et al* [4].

Table I
Subdomain properties

Subdomain	Conductivity (S/m)	Relative Permittivity
Blood	0.46	80
Muscle	0.16	11,800
Surroundings	0.10	80
Catheter (polyimide)	10^{-12}	2

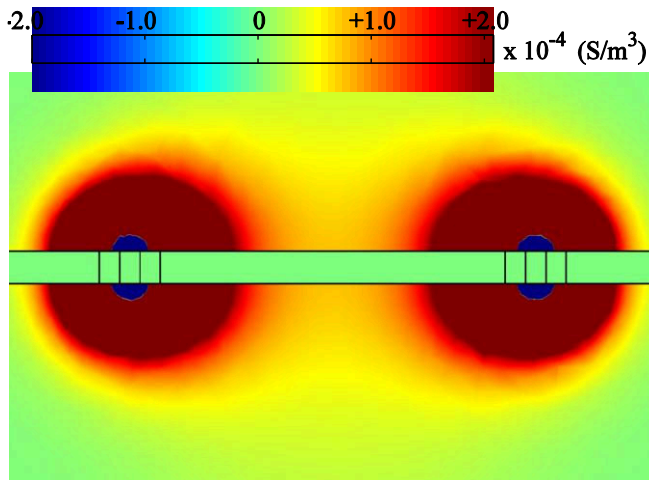


Fig. 2. Product of impedivity and sensitivity for the mouse catheter in a uniform field. The linear scale is allowed to saturate to show the negative sensitivity zones.

III. RESULTS

A. Murine Catheter without Surroundings

Analysis of the mouse catheter in a uniform field is shown in Fig. 2. This formulation shows the spatial contributions to

the total admittance, the integrand in equation 8 (the impedivity-sensitivity product). The integrand is the product of the local impedivity and sensitivity. Changes in the measured admittance due to variations in local properties are determined by the local sensitivity. Results show the measurement is heavily weighted by the regions in close proximity to the electrodes. Small negative sensitivity fields (blue) are located in the regions between the pairs of current carrying and voltage sensing electrodes.

The impedivity-sensitivity product in the mouse LV is shown at 15 μL in Fig. 3 to visually emphasize the removal of muscle using the admittance method. Prior to removal of the muscle signal, the muscle domain clearly contributes to the measurement. Following removal using the admittance method, the contribution of the muscle domain is greatly reduced (darker gray).

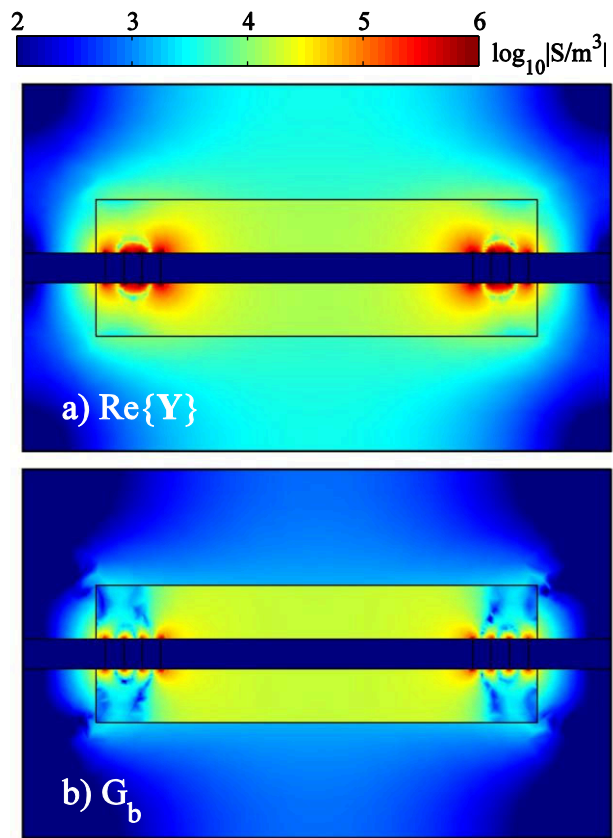


Fig. 3. Product of impedivity and sensitivity (top) and the product of G_b and sensitivity (bottom) at 15 μL .

The relative contributions of each segmental volume in the blood cavity at various volumes are shown in Fig. 4. Each point corresponds to the integration over a cylinder with a radius equal to the blood pool and a height of 0.25 mm, swept across the long axis of the LV.

As expected, the greatest sensitivity is located near the electrodes. The contribution of volumes between the electrodes is comparable throughout the cardiac cycle.

Volume vs. G_b is plotted in Fig. 5. Points correspond to the data from Table 2 and the line is Wei's equation calibrated using the 15 μL and 60 μL data points. The Geselowitz and

admittance methods produce nearly identical results.

Hypertonic saline simulations result in a parallel conductance of 470 μS , larger than the true parallel conductance from the Geselowitz relation. The least squares fit results to the end-systolic and end-diastolic conductance is $G_{\text{ES}}=0.43805 \cdot G_{\text{ED}}+264.36$, with $R^2 = 0.99998$.

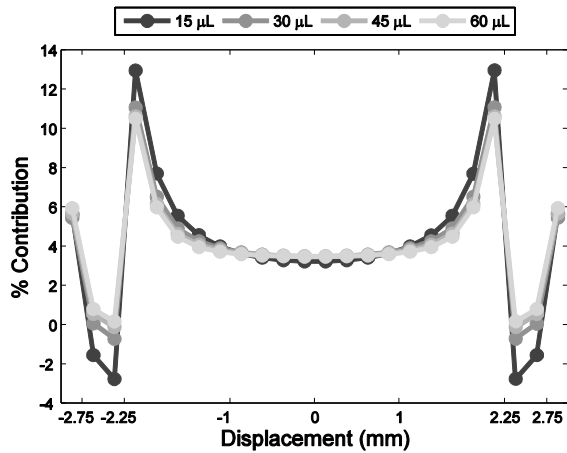


Fig. 4. Percent contribution to G_b vs. displacement showing the nonuniform sensitivity.

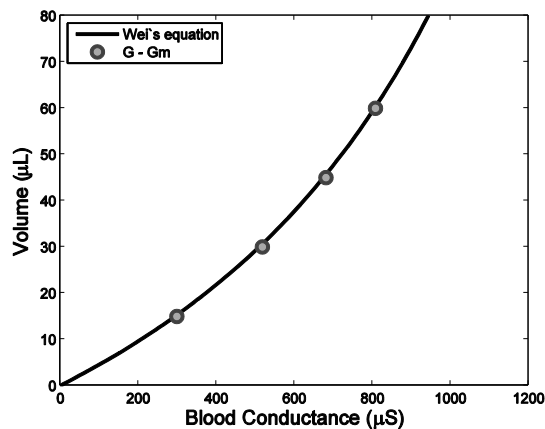


Fig. 5. Wei's equation fit to the G_b data from the mouse catheter with no surroundings. Calibration is applied using the SV and G_b data between 15 and 60 μL .

Table II
Mouse Model Results

Volume (μL)	Admittance Method		Geselowitz Relation	
	G_b (μS)	G_m (μS)	G_b (μS)	G_m (μS)
15	298.4	344.6	298.7	344.3
30	517.8	260.8	518.7	259.9
45	680.7	194.3	682.1	192.8
60	807.3	143.7	809.1	141.9

IV. CONCLUSION

Spatial sensitivity analysis of the admittance method was performed using the Geselowitz relation formulated for complex media. The murine conductance catheter exhibits the highest sensitivity near the stimulating and sensing electrodes. Negative sensitivity zones exist between each pair of stimulating and sensing electrodes.

Model results show that the admittance method correctly

removes parallel conductance and that the hypertonic saline method overestimate parallel conductance throughout the cardiac cycle. G_b errors using the admittance method are due to the true model being a mixture of parallel and series combinations of blood and muscle. Agreement between G_b from the admittance method and Geselowitz relation shows that the conductance catheter sensing domains are accurately represented by a parallel model. Further analysis quantifies the nonlinear sensitivity along the catheter, showing the highest sensitivity near the electrodes that does not change significantly over the cardiac cycle.

Wei's equation correctly fits G_b , showing that the equation is not affected by changes to the field geometry due to the presence of the myocardium.

Traditional interpretation of conductance catheter measurements assumes sensitivity is confined to the area between the voltage sensing electrodes. Catheter design may be evaluated using the Geselowitz relation to develop new configurations that distribute sensitivity more uniformly.

ACKNOWLEDGMENT

The authors would like to thank Dr. Jon Valvano, Dr. John Porterfield, and Kathryn Loeffler for their comments and suggestions.

REFERENCES

- [1] J. Baan, J. Koops, E. T. Vandervelde *et al.*, "Dynamic Absolute Left-Ventricular Volume Measured with the Conductance Catheter," *Circulation*, vol. 64, no. 4, pp. 177-177, 1981.
- [2] C. L. Wei, J. W. Valvano, M. D. Feldman *et al.*, "Volume catheter parallel conductance varies between end-systole and end-diastole," *IEEE Transactions on Biomedical Engineering*, vol. 54, no. 8, pp. 1480-1489, 2007.
- [3] C. Constantinides, S. I. Angeli, and R. J. Mean, "Murine Cardiac Catheterizations and Hemodynamics: On the issue of Parallel Conductance," *IEEE Transactions on Biomedical Engineering*, vol. 58, no. 11, pp. 3260-3268, Nov, 2011.
- [4] K. Raghavan, J. E. Porterfield, A. T. G. Kottam *et al.*, "Electrical Conductivity and Permittivity of Murine Myocardium," *IEEE Transactions on Biomedical Engineering*, vol. 56, no. 8, pp. 2044-2053, Aug, 2009.
- [5] B. R. Epstein, and K. R. Foster, "Anisotropy in the dielectric-properties of skeletal-muscle," *Medical & Biological Engineering & Computing*, vol. 21, no. 1, pp. 51-55, 1983, 1983.
- [6] J. E. Porterfield, A. T. G. Kottam, K. Raghavan *et al.*, "Dynamic correction for parallel conductance, $G(P)$, and gain factor, α , in invasive murine left ventricular volume measurements," *Journal of Applied Physiology*, vol. 107, no. 6, pp. 1693-1703, Dec, 2009.
- [7] S. Grimnes, and O. G. Martinsen, "Sources of error in tetrapolar impedance measurements on biomaterials and other ionic conductors," *Journal of Physics D-Applied Physics*, vol. 40, no. 1, pp. 9-14, Jan 7, 2007.
- [8] D. B. Geselowitz, "Application of electrocardiographic lead theory to impedance plethysmography," *Ieee Transactions on Biomedical Engineering*, vol. BM18, no. 1, pp. 38-&, 1971.
- [9] J. Lehr, "Vector derivation useful in impedance plethysmographic field calculations," *IEEE Transactions on Biomedical Engineering*, vol. BM19, no. 2, pp. 156-&, 1972, 1972.
- [10] C. L. Wei, J. W. Valvano, M. D. Feldman *et al.*, "Nonlinear conductance-volume relationship for murine conductance catheter measurement system," *IEEE Transactions on Biomedical Engineering*, vol. 52, no. 10, pp. 1654-1661, Oct, 2005.
- [11] X. M. Gao, A. M. Dart, E. Dewar *et al.*, "Serial echocardiographic assessment of left ventricular dimensions and function after myocardial infarction in mice," *Cardiovascular Research*, vol. 45, no. 2, pp. 330-338, Jan 14, 2000.